Evolution of a Pinch Column During the Acceleration of Fast Electrons and Deuterons in a Plasma-Focus Discharge

Pavel Kubes, Marian Paduch, Marek Jan Sadowski, Jakub Cikhardt, Balzhima Cikhardtova, Daniel Klir, Jozef Kravarik, Vojtech Munzar, Karel Rezac, Elzbieta Skladnik-Sadowska, Andrzej Szymaszek, Krzysztof Tomaszewski, Dobromil Zaloga, and Ewa Zielinska

***Abstract*— Plasma in a pinch column, as produced by a plasma-focus discharge at the deuterium filling and the current intensity reaching 1 MA, was investigated at the total neutron yield reaching about 10^{10} per discharge. The use was made of neutron diagnostics, laser interferometry, soft X-ray measurements, optical emission spectroscopy, magnetic probes, as well as electron and ion measurements with the temporal, spatial, and energetic resolutions. The detailed studies showed the ordered toroidal, helical, and plasmoidal structures which could contain currents with poloidal and toroidal components and their associated magnetic fields. Their spontaneous transformations were explained by changes in a topology of magnetic field lines due to magnetic reconnections. A nonthermal acceleration of fast electrons and ions (producing hard X-rays and fusion neutrons, respectively) corresponded to: 1) the formation of plasmoids in the pinch column and 2) a decay of pinch constrictions and secondary plasmoids during the evolution of instabilities. A filamentary structure of the current flow could explain the high energy density and fast transformations of the magnetic energy into kinetic energy of electron and ion beams (reaching energy of hundreds of kiloelectronvolt). This paper summarizes the results obtained with the PF-1000 facility in 2009–2017, and describes the internal transformations in a dense plasma column during the evolution of MHD instabilities.**

***Index Terms*— Dense plasma focus, magnetic reconnection, neutron source, self-generation.**

I. Introduction

Z-PINCHES and their alternative forms the dense plasma-focus discharges can efficiently accelerate electron and ion beams to high energies ranging up to hundreds of kiloelectronvolts, mainly during disruptions of the dense plasma column. In discharges with the deuterium filling, the hard X-rays (HXRs) and fast neutrons (produced by D–D fusion reactions) supply an indirect information about fast electrons and deuterons, and particularly about instants of their production, directions of their motion, and energies. The characteristics of the *Z*-pinch and plasma-focus discharges and different models of the fast particle acceleration were described in detail in [1]–[8]. In research on space and fusion plasmas, the magnetic reconnection was often indicated as a source of the fast electron and ion beam acceleration [9]–[12]. The experimental studies with the PF-1000 device showed the existence of ordered structures and filamentary forms of the current flow. This paper summarizes the basic phases of the pinch column evolution, and particularly MHD instability development during the period of the dominant fast electrons and ions acceleration induced by transformations of the local magnetic fields.

II. Experimental Facility

The reported studies were performed with the PF-1000 facility constructed at the Institute of Plasma Physics and Laser Microfusion, Warsaw, Poland, and operated mostly with the deuterium filling [13], [14]. The first specific feature of this device was the horizontal orientation of the electrode system, which made it possible to record fusion-produced neutrons by means of scintillation detectors in the same axial and radial distances from the pinch center. It enabled a simpler description of the neutron production to be made. The second specific feature of this device was relatively large dimensions of coaxial electrodes, which were not optimized for the maximal neutron yield. It ensured the formation of a plasma column of about 10 cm in length and an electron density of 10^{24}–10^{25} m^{-3}, transparent for an interferometry using the visible radiation from a diagnostic laser. Velocities of plasma column transformations, which reached (1–2) $\times$ 10^5 m/s, made it possible to perform detailed diagnostic measurements

Manuscript received April 28, 2018; revised July 11, 2018 and September 3, 2018; accepted October 2, 2018. Date of current version January 8, 2019. This work was supported in part by the Research Program under Grant MSMT LTT17015, Grant LTAUSA17084, Grant CZ.02.1.01/0.0/0.0/16_019/0000778, Grant GACR 16-07036S, and Grant IAEA CRP *RC*-19253, in part by SGS under Grant 16/223/OHK3/3T/13, and in part by the Polish Ministry of Science and Higher Education within a framework of the financial resources allocated in 2018 for the realization of the international co-financed projects. The review of this paper was arranged by Senior Editor F. Beg. *(Corresponding author: Pavel Kubes.)*

P. Kubes, J. Cikhardt, B. Cikhardtova, D. Klir, J. Kravarik, V. Munzar, and K. Rezac are with the Department Physics, Faculty of Electrical Engineering, Czech Technical University, 166-27 Prague, Czech Republic (e-mail: kubes@fel.cvut.cz).

M. Paduch, A. Szymaszek, and E. Zielinska are with the Institute of Plasma Physics and Laser Microfusion, 01-497 Warsaw, Poland.

M. J. Sadowski is with the Institute of Plasma Physics and Laser Microfusion, 01-497 Warsaw, Poland, and also with the National Centre for Nuclear Research (NCBJ), 05-400 Otwock, Poland.

E. Skladnik-Sadowska and D. Zaloga are with the National Centre for Nuclear Research (NCBJ), 05-400 Otwock, Poland.

K. Tomaszewski is with ACS Ltd., 01-497 Warsaw, Poland.

Digital Object Identifier 10.1109/TPS.2018.2874288

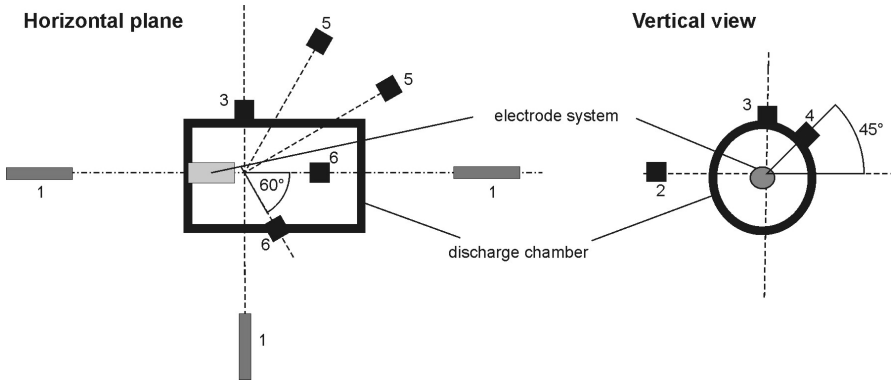

Fig. 1. Scheme of the diagnostics arrangement: 1—scintillation detectors, 2—laser interferometer frame, 3—p-i-n detector, 4—SXR framing camera, 5—Ag activation detectors, and 6—ion pinhole cameras.

with nanosecond-temporal and millimeter-spatial resolutions. The third specific feature of the described facility was the laser interferometry system, which enabled to investigate the pinch internal structure by recording 15 frames during each discharge, i.e., to visualize the evolution of internal structures inside the plasma column in each individual shot, from the radial implosion phase until the plasma decay.

The PF-1000 facility was equipped with the Mather-type coaxial electrodes of 480 mm in length. The anode was made of a copper tube of 230 mm in diameter. The cathode of 400 mm in diameter consisted of 12 stainless-steel tubes (each of 80 mm in diameter) distributed symmetrically around the z-axis. During the described experiments, the main capacitor bank was charged to (16–20) kV, and it stored energy of (250–350) kJ, respectively. The peak current intensity reached (1–2) MA, but during the pinch phase, it decreased to about (0.7–1.5) MA. Both decrease were the consequence of the reduction of the initial charging voltage of the condenser bank during subsequent experimental campaigns in the past years. The scheme of diagnostics is presented in Fig. 1. The voltage, the current-derivative, and the total-current traces were measured at the main current collector. Time-resolved soft X-ray (SXR) signals in the photon energy range of (0.7–15) keV were recorded with a 3-ns temporal resolution by means of a silicon p-i-n diode filtered by a 10-μm-thick Be foil. Three scintillation detectors were used to record HXR and neutron signals in both axial and side-on directions, at the same total distances of 7 m from the pinch center, with a 3-ns resolution. They enabled to determine instants of the emission of HXRs and fusion-produced neutrons as well as to estimate their energies [15]. The interferometric frames were obtained by means of 2-ns laser pulses with mutual delays equal to 10 or 20 ns and they imaged the plasma distribution with a spatial uncertainty of 1 mm [16]. The laser interferometer had the radial (side-on) line of sight in the horizontal plane, and it used parallel mirrors, which gave widely distributed interferometric fringes from shots without plasma. For shots with plasma, the interferometer recorded many interferometric fringes, which enabled the spatial distribution of the electron density to be determined. The closed dense interferometric fringes indicated regions of the extreme plasma density. The electron densities were calculated using the Abel transformation, i.e., a mathematical procedure of the inversion of an integral equation which describes a dependence of the recorded shifts of interferometric fringes on a plasma refractive index in the observation plane. This procedure makes it possible to calculate a distribution of the electron density, under the assumption of the azimuthal symmetry of the pinch column [17], [18] The absolute calibrated magnetic probes made it possible to estimate the azimuthal and axial components of a local magnetic field of the order of several teslas [19]–[21].

Intensities of spectral lines of H- and He-like ions of impurities (O, N, and C), which were measured by means of the vacuum ultraviolet radiation emission spectroscopy, enabled evaluations of an average electron temperature $T_e = (50–150)$ eV to be performed [22]. The measurements of the electron temperature, which were carried out by means of filtered p-i-n diodes recording SXR pulses, showed that the local values of T_e could reach even hundreds of electron-volts [23], [24]. Sources of the fast deuterons were investigated by an analysis of the time-integrated deuteron-tracks recorded upon plastic detectors placed inside the ion pinhole cameras, which were located in front of the anode end plate, at angles ranging (0°–60°) to the z-axis. Different filters placed upon the track applied detectors made it possible to select deuterons of different energies, and to estimate their deflections in the magnetic fields [25]. The total neutron yield was measured by means of two calibrated silver-activation counters. The peak of the current-derivative dip was assigned as the instant $t = 0$. An uncertainty in the timing of different waveforms recorded with the digital oscilloscope during a single discharge was about (3–5) ns. This uncertainty was mainly caused by response times of the scintillation detectors and photomultipliers.

III. Organized Structures Inside the Pinch Column During the Fusion Neutron Production

The recorded HXR pulses were evidently generated during interactions of fast electrons with electrode and chamber walls. The fusion neutrons were born during collisions of the fast deuterons by the beam-target mechanisms. Energy distributions of HXRs and deuterons had relatively wide spectra. The energy spectrum of fast electrons measured upstream by means

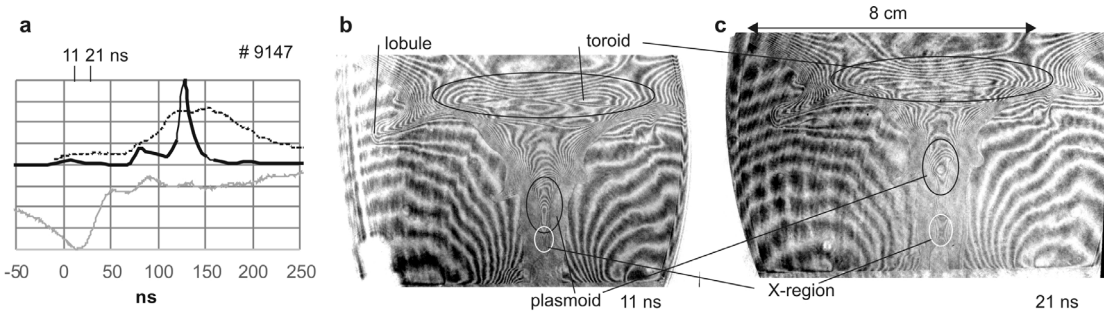

Fig. 2. Data from shot #9147. (a) Waveforms of the current-derivative (gray), HXRs (black), and fusion neutrons (dashed) as a function of time. The neutron signals recorded side-on have been shifted back in time under assumption that neutrons energy was 2.45 MeV. The numbers above the waveforms showed the instants of recording of interferometric frames. The "y" scale in arbitrary units made it possible to compare the temporal evolution of presented signals. The interferometric images showed: (b) three basic structures inside the pinch column (i.e., plasmoid, toroid, and lobule) and X-region and (c) transformation of the pinch column after 10 ns, with an axial shift of the plasmoid.

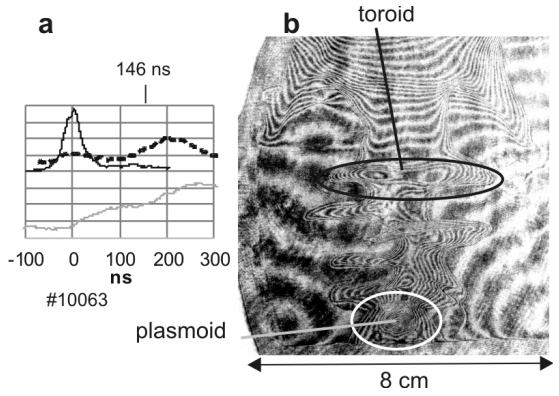

Fig. 3. Data from shot #10063. (a) Waveforms of the current-derivative (gray), HXRs (black), and fusion neutrons (dashed) as a function of time. The neutron signals recorded side-on have been shifted back in time under assumption that neutrons energy was 2.45 MeV. The number above the waveforms corresponded to the instant of recording of the interferometric frame. (b) Interferometric frame showed the internal distribution of a plasma line density during the evolution of the MHD instability. Some temporal shift was caused by the zippering of the plasma column, starting from the anode toward the higher z regions.

of a Thomson-type spectrometer installed at the PF-1000 facility had the maximum in the range from 100 to 200 keV [26]. The fast deuterons producing D–D fusion neutrons (estimated on the basis of their times of flight to the axial scintillation detectors) have values in the range of 50–500 keV. It should, however, be noted that in the most shots, the deuterons producing neutrons had dominant energies downstream (100–200) keV also. Two HXR and neutron peaks, which were observed in the most discharges, corresponded to two phases of the plasma column transformation. The first weaker pulses were emitted at the stopping of the plasma sheath implosion (see Fig. 2).

The second (often dominant) pulses were generated during the phase of instabilities development, at the interruption and decay of a part of the dense pinch column (see Figs. 3 and 4).

The applied laser interferometry made it possible to estimate a distribution of the line electron density in the observed internal structures, and to correlate their evolution with instants of the neutron production [27].

The stopping phase of the dense plasma compression corresponded to the minimal pinch diameter and the extreme values of the voltage and current-derivative signals. The first HXR and fusion neutron signals [shown in Fig. 2(a)] documented the acceleration of fast electrons and deuterons.

The interferometric image [presented in Fig. 2(b) and (c)] showed the existence of three types of the structures: plasmoidal-, toroidal-, and lobule-like structures. The initial phase of a plasmoid formation was imaged with the closed interferometric fringes visible in Fig. 2(b) and (c). In this phase, the plasmoid constituted the plasma region of a considerable higher density. The number of plasma particles inside this plasmoid was increased by a confinement of plasma flowing from the z-axis surrounding [shown in Fig. 2(b) and (c) as the X-shaped fringe regions marked by white ellipses]. The radial and axial profiles of plasma density were the Gaussian ones, as reported in [27]. The maximal plasma density in the plasmoid center reached about 10^{25} m^{-3}. The plasmoid was formed at the axial position of a smaller plasma lobule of the former toroid. During the formation of the plasmoid one could observe some internal coalescence of plasma turbulences [28]. The internal density gradients in the ordered structures (with the noticeable symmetry) could be caused by the internal closed currents.

The presence of the axial magnetic components inside and outside the dense plasma column was confirmed by the signals obtained from miniature absolutely calibrated magnetic probes [20], [21]. It was deduced that the plasmoid was compressed by the pressure of external currents flowing along the column surface. Its compactness and internal links facilitated, for example, the formation of the plasmoid around an Al wire which was placed along the z-axis [29].

The toroidal plasma structure could be formed by some internal toroidal currents. The pressure of the expanding internal poloidal magnetic field limited the pinching of the main discharge current. It caused an increase in a diameter of the plasma column and produced some distinct lobules.

The upper toroidal structure, which was marked by a black ellipse in Fig. 2(b), had the maximum plasma density in the center of the closed interferometric fringes. This structure separated the pinch column from the umbrella-shaped plasma

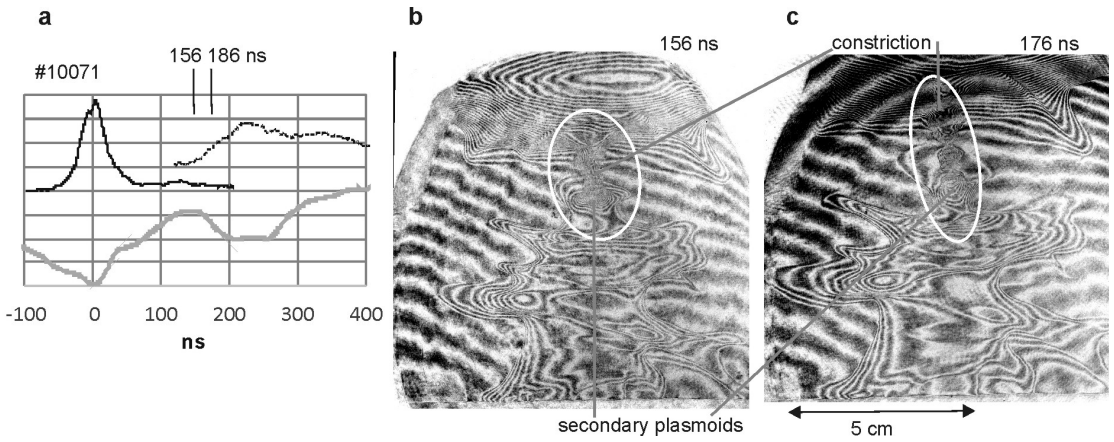

Fig. 4. Data from shot #10071. (a) Current-derivative (gray), HXRs (black), and fusion neutrons (dashed) as a function of time. The neutron signal recorded side-on has been shifted back in time under assumption that neutrons energy was 2.45 MeV. The numbers above the waveforms indicated instants of recording of the interferometric frames. (b) and (c) Interferometric images of successive transformations of the pinch constriction into the secondary plasmoids and necks between them (marked by white ellipses).

sheath, and it was accompanied by the distinct plasma lobule side-on. The considered structure was formed in an early phase of the plasma implosion, and it played a significant role in the dynamics of the pinched column. The shape of the top of the lobule could suggest some transport of the mass between the dense plasma column and its low-density surrounding.

The described behavior could also lead to an interpretation which assumed the existence of a closed current external to the dense column, which shifts the discharge current far from the pinch column. Its magnetic field could also transport the pinching pressure from the discharge current upon the pinch column surface [25].

The interferometric image presented in Fig. 2(c) has shown the three important transformations of the plasma column, which occurred during 10-ns period.

1) The diameter of the plasma toroid was slightly decreased, probably due to an increase in the poloidal current component.
2) There appeared an axial shift and an increase in the plamoid volume.
3) The X-region dimensions were increased, due to some absorption of plasma by the growing plasmoid.

Experimental results from later phases of PF-1000 discharges supplied more information about plasma dynamics (see Fig. 3).

During the next phase of the pinch evolution some stagnation of the dense column was observed. It was characterized by the regions of the dense plasma column without any internal fringes and density gradients. The first plasmoid moved toward the top of the dense plasma column with a velocity equal to about 10^5 m/s, as a consequence of the inertia of confined plasma at its formation [see Figs. 2(b) and (c)] [28]. In the later phase, the stagnated plasma column was subjected to the development of the strong MHD instability. It was started by some stratification of the smooth plasma surface and was continued by the implosion of its parts (constrictions) towards the z-axis. That evolution was temporally spread out by the zippering of the dense pinch column. This phase was documented by the image shown in Fig. 3(b) One could see the later phase near the anode end, and the earlier one at higher z regions. This transformation was accompanied by an axial transport of plasma from the imploding constrictions into the neighboring structures: first—into a wider toroid (marked by the black ellipse in Fig. 3(b), and later on—into developing plasmoids (marked by the white ellipse). The mass and density inside the described structures increased considerably, and the kinetic energy of confined plasma moving along and across the magnetic lines was transformed into the magnetic energy, similarly as described in the previous paragraph.

Data shown in Fig. 4 presented the final phase of the evolution of the plasma constriction during the period of the neutron production. It was started by the second stratification of the plasma column surface along its length [see Fig. 4(b)], and it was continued by the formation of the secondary plasmoids and necks (short constrictions) between them (see Fig. 4(c)], analogically to a cascade development of $m = 0$ instability in an X-pinch experiment [31]. A decay phase of the constriction (realized by the absorption of plasma by the plasmoid), as well as the decays of the secondary plasmoids (realized by their expansion) were going on during the generation of the second dominant neutron signal, as one can see in Fig. 4(a). A longer production of the fusion-produced neutrons corresponded to the decay of the observed plasmoids, during which their magnetic energy was released, as one can see in Figs. 3(b), 4(b), and 4(c) [28], [30]. It should be noted that in the recorded interferometric fringes, there was no experimental information about the acceleration of fast charged particles in the interrupted pinch region (filled up with low-density plasma). Such a possibility in Z-pinch discharge was discussed (see [8]).

In the reported PF-1000 experiments, the transformations of the described toroidal and plasmoidal structures were examples of a spontaneous evolution of the organized plasma structures. It was caused by the magnetic dynamo and magnetic reconnections observed also in other plasmas [10]. Plasma of the parameters described above was a convenient medium for the self-organization and self-generation of a magnetic

field, because of relatively high Reynolds magnetic numbers (ratio of frozen and dissipative characteristics [4]) which reached 10^3. A scenario of the evolution of the ordered structures was described in [28] and [32]. The process was started by some concentration of a spontaneously generated azimuthal current component into the toroidal structure. The confinement of plasma incoming into the toroid (along and across the magnetic lines) was accompanied by the transformation of the kinetic energy into the chaotic turbulence inducing the formation of magnetic multipoles. The following self-organization increased gradually the initially weak poloidal current component, which transformed the toroidal structure into the plasmoid [see Figs. 2(b) and (c)]. The poloidal current in the plasmoid could be oriented as the main discharge current, from the anode near boundaries of the plasmoid and in the opposite direction (toward the anode) in the axial region. This scenario described the transformation occurring at the evolution of the MHD instability also. The observed long-living first plasmoids, which were formed during the first neutron pulse, remained the quasi-stable structures with probably balanced poloidal and toroidal current components (similar to a spheromak), as one can see in Figs. 2(b) and (c) and up in Fig. 4(b). In the secondary plasmoids, which were formed during the plasma constriction compression at higher velocities and intensities, the ratio of the poloidal and toroidal current components could be higher than that in a balanced form, and the central parts of those plasmoids were subjected to the pinching [33]. This process was accompanied by the evolution of instabilities leading to a partial decay of the closed internal currents and fast transformations of the magnetic energy into energy of the fast ion beams.

The relaxation time of the electron and ion temperatures, at the electron densities of about 3×10^{24} m^{-3} and electron temperatures equal to 50–150 eV, should be of order of 10 ns [4]. Consequently, one might assume the achievement of the quasi-stationary conditions at the observed slower transformations which occurred in plasma during several tens of nanoseconds. At these specific conditions in the PF-1000 facility, the computed distribution of the plasma pressure made it possible to estimate mean values of the magnetic pressure and magnetic field in the described ordered structures. In those calculations, the repulsive plasma pressure of the toroid or plasmoid was compensated by the pinching pressure of the current flowing through the plasma column surface layer. It was in a good agreement with the virial theorem [34]. A mean value of the magnetic field amounted to about 5 T, and the corresponding current intensity reached several tens of kiloampheres in the toroidal structures and hundreds of kiloampheres in plasmoidal structures [22]. That value of the magnetic field was consistent with the result of time-resolved measurements performed with calibrated magnetic probes [19]–[21].

The formation and evolution of the organized toroidal and plasmoidal structures were investigated at different filling gases: hydrogen, deuterium, helium, nitrogen, and neon. In the hydrogen discharges such structures were formed after a long time (hundreds of nanoseconds) and their final shapes were irregular. In the helium or nitrogen discharges the formation of the considered structures was going also during a longer period, but their surfaces were more regular and smooth. Also their stability was higher, and the duration of their transformations was longer than that in deuterium, and reached hundreds of nanoseconds [35], [36]. Consequently, the deuterium filling was the best for the formation and transformation of the ordered and regular structures lasting several tens of nanoseconds, and decaying during the similar period. At the deuterium filling, the total neutron yield corresponded to the duration of the plasmoids decay. The higher neutron yields were observed at the faster decay of those plasmoids.

It should be noted here that the transformation velocity observed in the recorded interferometric frames, i.e., the velocity of the compression or expansion of the plasma column, and that of the structure evolution, corresponded to the Alfvén velocity which was equal to $(1–2) \times 10^5$ m/s. That velocity was too low to explain energies of the fast electrons and ions, which produced the recorded HXR and neutron pulses, respectively. The energy values ranging hundreds of kiloelectronvot might be achieved at the filamentary structure of the current.

It is well known that current flows in PF-discharges have often a filamentary structure, and the primary quasi-linear filaments connect the anode with the cathode [2]. In many experiments, it was shown that the current filaments can exist in the plasma sheath during its acceleration as well as during its radial compression [37]. In earlier PF-1000 experiments, it was observed that local magnetic fields combined with the current filaments deflected trajectories of charged particles (fast ions and fusion-produced protons) and influenced their spatial distributions [40], [41]. Not only the distinct traces of the primary current filaments upon the anode surface were observed after a single discharge, but also they were recorded after many discharges [32], what proved their good reproducibility. It should be added that the fine structure of the current filaments might be more complex, and the plasma filaments could have also some azimuthal and radial components. Tiny current filaments observed in the PF-1000 experiments were described in [40] and [41]. Those filaments, which connected external layers of the dense plasma column with the internal plasmoids, were interpreted as a visualized transport of the current and energy between these regions, mainly during the period of the neutrons production. One could also consider the current flow inside toroidal plasma tubes in the form of several filaments with the dominant toroidal components. On the contrary, the current filaments in the plasmoids had probably the dominant poloidal components with some stabilizing toroidal components along their length. Consequently, the transformations of the toroidal and plasmoidal structures might be a result of some reconnections of those filaments. A decay of the plasmoid might also be explained, as mentioned above, as a decay of some pinched current filaments, first in their centers. A scenario of the possible reconnections was described in [36]. It explained the acceleration of fast particles by the induction of the strong electric fields during the rapid annihilation of strong local magnetic fields of filaments, ranging hundreds T. The hot-spots, i.e., sub-millimeter structures, which emit the intense X-rays

during the evolution of instabilities in plasmas composed of higher z elements, can also be interpreted as the results of a release of the magnetic energy from regions of a high energy density. This concept of micropinches, as described in [31] and [40], corresponds to the plasma nodules described by Bostick [41]. In discharges performed at the deuterium filling such microstructures could be more stable due to the limitation of radiative losses. They could decay and induce the acceleration of charged particles. Energy density inside these structures, characterized by the kinetic energy of deuterons about 200 keV and plasma density of about 3×10^{24} m^{-3}, corresponded to the magnetic field of about 500 T.

Plasma regions emitting the fast deuterons were investigated by means of ion pinhole cameras equipped with the plastic nuclear-track detectors. It was found that the fast deuterons were emitted mainly from two regions [25]. The first region, located near the pinch center, emitted the fast deuterons at angles ranging from 0°–60° to the z-axis. Those deuterons were probably emitted from the plasmoid during its transformation and a decay of current filaments. The second source, which was imaged as a ring region of the radius of about 3 cm, was situated outside of the dense column. The traces of recorded deuterons in the slant detector belong to the central region only, the traces of external rings absent.

It should be added that the smaller radius of the ring ion pinhole images corresponded to the position of plasma lobule tops. This region could contain axial currents flowing in both directions, as was mentioned above and discussed in [30]. A similar current configuration might be present also in the plasma layers of a larger diameter. Therefore, it could be concluded that the acceleration of the ion beams in both cases correlated with decays of the closed currents and accompanied magnetic fields. Energy of the accelerated ion beams amounted to several kilojoules, and it was higher than that contained in the volume of the magnetic field (which ranged about kilojoules). Hence, it was deduced that the acceleration was a more complicated process, in which the energy of the discharge current was delivered from the external current layers to the observed internal structures, also during the period of the fast particles acceleration [42], [43].

It should be mentioned here that simultaneous processes of the fast magnetic energy released from the organized plasma structures at the electron and ion beam accelerations were also discussed in other fusion and cosmic plasmas. It was found that laser beams focused upon the target foils produced a perpendicular intense plasma jet, which was investigated by the laser schlieren and interferometry, as well as the Faraday rotation techniques [12]. The results obtained from those measurements showed that in such jets there appeared currents ranging hundreds of kiloampheres, accompanied by magnetic fields of the order of 5 kT in the sub-millimeter regions. In the case of two laser beams focused nearby, both generated plasma jets (which had the same orientation of the current flow) attracted themselves. The coalescence of those organized structures was explained by magnetic reconnections occurring in the nanosecond time scale [11]. The X-rays and fusion neutrons observed in the NIF D–T fusion experiment were emitted from the toroidal-like plasma structure oriented perpendicular to the pellet axis [42]. In tokamak plasmas, the kinetic energy of particles delivered by the additional heating could also be transformed partly into the magnetic energy which disturbed the initially smooth magnetic surfaces. That the energy was periodically released in the form of the fast run-away electrons which were apparently generated by magnetic reconnections, and it allowed to reestablish the ordered and smooth magnetic surfaces [10]. The magnetic reconnections are considered also as mechanisms responsible for changes of a complicated topology of the magnetic field in solar flares [45]. In this case the SXR and corpuscular observations indicated very fast transformations of the magnetic energy into kinetic one (of fast charged particles), and into the heating in the solar chromosphere and corona. It should be mentioned that for solar plasma, the MHD modeling of the magnetic reconnections has already been performed at the simplifying conditions, but for Z-pinches, the detailed modeling of such phenomena has not provided so far.

IV. Conclusion

The investigation of the plasma produced within the PF-1000 facility, with convenient values of the plasma density and velocity of transformations—made it possible to study its transformations, which were accompanied by the acceleration of the charged particles, mainly during the evolution of MHD instabilities. It was found that in the plasma pinch column, there exist spontaneously generated ordered structures. Their composition could be explained by the closed internal and external currents and their magnetic fields. The currents could have the filamentary forms, and their transformations might be described by the magnetic reconnections, which in turn might also explain the fast particles acceleration.

The described studies of the internal structures and their transformations observed within the PF-1000 discharges have shown the complexity of physical processes in dense magnetized plasmas. These processes require further experimental and theoretical studies, including detailed computer simulations.

References

[1] M. G. Haines, "A review of the dense Z-pinch," *Plasma Phys. Controlled Fusion*, vol. 53, no. 9, p. 093001, 2011.
[2] A. Bernard *et al.*, "Scientific status of plasma focus research," *J. Moscow Phys. Soc.*, vol. 8, pp. 93–170, Nov. 1998.
[3] D. D. Ryutov, M. S. Derzon, and M. K. Matzen, "The physics of fast *Z* pinches," *Rev. Mod. Phys.*, vol. 72, pp. 205–223, Jan. 2000.
[4] D. D. Ryutov, "Characterizing the plasmas of dense *Z*-pinches," *IEEE Trans. Plasma Sci*, vol. 43, no. 8, pp. 2363–2384, Aug. 2015.
[5] L. Soto, "New trends and future perspectives on plasma focus research," *Plasma Phys. Controlled Fusion*, vol. 47, pp. A361–A381, Apr. 2005.
[6] V. I. Krauz, "Progress in plasma focus research and applications," *Plasma Phys. Controlled Fusion*, vol. 48, pp. B221–B229, Nov. 2006.
[7] M. Krishnan, "The dense plasma focus: A versatile dense pinch for diverse applications," *IEEE Trans. Plasma Sci.*, vol. 40, no. 12, pp. 3189–3221, Dec. 2012.
[8] D. Klir *et al.*, "IoN acceleration mechanism in mega-ampere gas-puff Z-pinches," *New J. Phys.*, vol. 20, p. 053064, May 2018.
[9] H. K. Park *et al.*, "Observation of high-field-side crash and heat transfer during sawtooth oscillation in magnetically confined plasmas," *Phys. Rev. Lett.*, vol. 96, p. 195003, May 2006.
[10] M. Yamada, R. Kulsrud, and J. Hantao, "Magnetic reconnection," *Rev. Mod. Phys.*, vol. 82, pp. 603–664, Mar. 2010.

[11] P. M. Nilson *et al.*, "Magnetic reconnection and plasma dynamics in two-beam laser-solid interactions," *Phys. Rev. Lett.*, vol. 97, p. 255001, Dec. 2006.
[12] T. Pisarczyk *et al.*, "Kinetic magnetization by fast electrons in laser-produced plasmas at sub-relativistic intensities," *Phys. Plasmas*, vol. 24, p. 102711, Oct. 2017.
[13] M. Scholz, L. Karpiński, M. Paduch, K. Tomaszewski, R. Miklaszewski, and A. Szydlowski, "Recent progress in 1 MJ plasma-focus research," *Nukleonika*, vol. 46, no. 1, pp. 35–39, 2001.
[14] M. Sadowski and M. Scholz, "Results of large scale plasma-focus experiments and prospects for neutron yield optimization," *Nukleonika*, vol. 47, no. 1, pp. 31–37, 2002.
[15] K. Rezac, D. Klir, P. Kubes, and J. Kravarik, "Improvement of time-of-flight methods for reconstruction of neutron energy spectra from D(d,n)^{3}He fusion reactions," *Plasma Phys. Controlled Fusion*, vol. 54, no. 10, p. 105011, 2012.
[16] E. Zielińska, M. Paduch, and M. Scholz, "Sixteen-frame interferometer for a study of a pinch dynamics in PF-1000 device," *Contrib. Plasma Phys.*, vol. 51, pp. 279–283, Mar. 2011.
[17] *Abel Transform*. [Online]. Available: https://en.wikipedia.org/wiki/Abel_transform
[18] R. H. Huddlestone and S. L. Leonard, *Plasma Diagnostic Techniques*. New York, NY, USA: Academic, 1965.
[19] V. Krauz *et al.*, "Experimental study of the structure of the plasma-current sheath on the PF-1000 facility," *Plasma Phys. Controlled Fusion*, vol. 54, no. 2, p. 025010, 2012.
[20] V. I. Krauz *et al.*, "Experimental evidence of existence of the axial magnetic field in a plasma focus," *Europhys. Lett.*, vol. 98, no. 4, p. 45001, 2012.
[21] P. Kubes *et al.*, "Correlation of magnetic probe and neutron signals with interferometry figures on the plasma focus discharge," *Plasma Phys. Controlled Fusion*, vol. 54, no. 10, p. 115005, 2012.
[22] P. Kubes *et al.*, "Transformation of the ordered internal structures during the acceleration of fast charged particles in a dense plasma focus," *Phys. Plasmas*, vol. 24, p. 072706, Jun. 2017.
[23] E. Skladnik-Sadowska *et al.*, "Research on soft X-rays in high-current plasma-focus discharges and estimation of plasma electron temperature," *Plasma Phys. Controlled Fusion*, vol. 58, no. 9, p. 095003, 2016.
[24] D. R. Zaloga, M. J. Sadowski, E. Skladnik-Sadowska, M. Paduch, E. Zielinska, and K. Tomaszewski, "Influence of gas conditions on electron temperature inside a pinch column of plasma-focus discharge," *J. Phys., Conf. Ser.*, vol. 959, no. 1, p. 012003, 2018.
[25] P. Kubes *et al.*, "Characterization of fast deuterons involved in the production of fusion neutrons in a dense plasma focus," *Phys. Plasmas*, vol. 25, p. 012712, Jan. 2018.
[26] E. Skladnik-Sadowska *et al.*, "Recent measurements of IoN- and electron-beams within PF-1000," in *Proc. ICDMP Workshop (IPPLM)*, Warsaw, Poland, 2009.
[27] P. Kubes *et al.*, "Spontaneous transformation in the pinched column of the plasma focus," *IEEE Trans. Plasma Sci.*, vol. 39, no. 1, pp. 562–568, Jan. 2011.
[28] P. Kubes *et al.*, "The evolution of the plasmoidal structure in the pinched column in plasma focus discharge," *Plasma Phys. Controlled Fusion*, vol. 58, no. 4, p. 045005, 2016.
[29] P. Kubes *et al.*, "Influence of the Al wire placed in the anode axis on the transformation of the deuterium plasma column in the plasma focus discharge," *Phys. Plasmas*, vol. 23, p. 062702, May 2016.
[30] P. Kubes *et al.*, "Existence of a return direction for plasma escaping from a pinched column in a plasma focus discharge," *Phys. Plasmas*, vol. 22, p. 052706, May 2015.
[31] S. A. Pikuz, T. A. Shelkovenko, and D. A. Hammer, "X-pinch. Part I," *Plasma Phys. Rep.*, vol. 41, no. 4, pp. 291–342, 2016.
[32] P. Kubes *et al.*, "Scenario of pinch evolution in a plasma focus discharge," *Plasma Phys. Controlled Fusion*, vol. 55, no. 3, p. 035011, 2013.
[33] P. Kubes *et al.*, "Increase in the neutron yield from a dense plasma-focus experiment performed with a conical tip placed in the centre of the anode end," *Phys. Plasmas*, vol. 24, p. 092707, Aug. 2017.
[34] V. D. Shafranov, *Theory of Plasma Physics*. Moscow, Russia: Gosatomizdat, 1963.
[35] P. Kubes *et al.*, "Interferometry and X-ray diagnostics of pinched helium plasma in a dense plasma focus with an AL-wire on the axis," *Phys. Plasmas*, vol. 23, p. 112708, Nov. 2016.
[36] P. Kubes *et al.*, "The influence of the nitrogen admixture on the evolution of a deuterium pinch column," *Phys. Plasmas*, vol. 23, p. 082704, Jul. 2016.
[37] M. Sadowski, H. Herold, H. Schmidt, and M. Shakhatre, "Filamentary structure of the pinch column in plasma focus discharges," *Phys. Lett. A*, vol. 105, no. 3, pp. 117–123, 1984.
[38] A. Malinowska *et al.*, "Measurements of ion micro-beams in RPI-type discharges and fusion protons in PF-1000 experiments," *Phys. Scripta*, vol. 2006, p. 104, Mar. 2006.
[39] M. J. Sadowski and M. Scholz, "The main issues of research on dense magnetized plasmas in PF discharges," *Plasma Source Sci. Technol.*, vol. 17, p. 024001, May 2008.
[40] V. V. Ivanov *et al.*, "Study of micro-pinches in wire-array Z pinches," *Phys. Plasmas*, vol. 20, p. 112703, Oct. 2013.
[41] W. H. Bostick, "The pinch effect revisited," *Int. J. Fusion Energy*, vol. 1, pp. 1–55, Mar. 1977.
[42] P. Kubes *et al.*, "Filamentary structure of plasma produced by compression of puffing deuterium by deuterium or neon plasma sheath on plasma-focus discharge," *Phys. Plasmas*, vol. 21, p. 122706, Nov. 2014.
[43] P. Kubes *et al.*, "Filamentation in the pinched column of the dense plasma focus," *Phys. Plasmas*, vol. 24, p. 032706, Feb. 2017.
[44] H.-S. Park *et al.*, "High-adiabat high-foot inertial confinement fusion implosion experiments on the national ignition facility," *Phys. Rev. Lett.*, vol. 112, p. 055001, Feb. 2014.
[45] M. Janvier, "Three-dimensional magnetic reconnection and its application to solar flares," *J. Plasma Phys.*, vol. 83, no. 1, p. 535830101, 2017.

Authors' photographs and biographies not available at the time of publication.